Initial Results for Automated Computational Modeling of Patient-Specific Electromagnetic Hyperthermia

Melinda J. Piket-May, *Student Member, IEEE,* Allen Taflove, *Fellow, IEEE,* Wei-Chung Lin, *Member, IEEE,* Daniel S. Katz, *Student Member, IEEE,* V. Sathiaseelan, *Member, IEEE,* and B. B. Mittal

***Abstract*—Developments in finite-difference time-domain (FD-TD) computational modeling of Maxwell's equations, supercomputer technology, and computed tomography (CT) imagery open the possibility of accurate numerical simulation of electromagnetic (EM) wave interactions with specific, complex, biological tissue structures. One application of this technology is in the area of treatment planning for EM hyperthermia. In this paper, we report the first highly automated CT image segmentation and interpolation scheme applied to model patient-specific EM hyperthermia. This novel system is based on sophisticated tools from the artificial intelligence, computer vision, and computer graphics disciplines. It permits CT-based patient-specific hyperthermia models to be constructed without tedious manual contouring on digitizing pads or CRT screens. The system permits in principle near real-time assistance in hyperthermia treatment planning. We apply this system to interpret actual patient CT data, reconstructing a 3-D model of the human thigh from a collection of 29 serial CT images at 10 mm intervals. Then, using FD-TD, we obtain 2-D and 3-D models of EM hyperthermia of this thigh due to a waveguide applicator. We find that different results are obtained from the 2-D and 3-D models, and conclude that full 3-D tissue models are required for future clinical usage.**

I. Introduction

Much evidence has emerged from clinical studies that hyperthermia, i.e., heating of tumors to temperatures greater than 42°C, has efficacy as an adjuvant to radiation therapy in the treatment of localized superficial malignancies [1]–[5]. However, a recent study by the Radiation Therapy Oncology Group has cast a shadow over the earlier promising results by showing no significant difference between complete response rates obtained with and without hyperthermia [6]. The principal reason for these poor results seems to be inadequate heating of the tumors, especially those larger than 3 cm in diameter due to poor coverage with external microwave applicators. In hyperthermia applications, adequacy of tumor coverage can reasonably be related to the extent to which the tumor is enclosed by surfaces of 50% iso-SAR (specific absorption rate, the absorbed power density in watts/kg) produced by the applicators.

The objective is to heat all tumor tissues of a patient to a uniform desired temperature without overheating surrounding normal tissues. However, this is difficult because current equipment and techniques produce poorly localized nonuniform heating in both tumor and normal tissues. This is further complicated by the cooling produced by significantly varying blood perfusion rates within the heated volumes. At present, heating techniques using electromagnetic (EM) energy are commonly employed in the clinic to produce therapeutic temperatures in tumors [7]. A number of factors influence the SAR patterns from commonly used EM applicators. Significant among these are: 1) the effect of relative applicator positioning with respect to the defined treatment volume; 2) the means of coupling the energy from the applicator(s) to the patient's surface; and 3) the complex, patient-specific tissue geometry. It is very difficult to either intuitively visualize or measure these effects, especially for deep tumor treatments where the SAR patterns are strongly affected by internal tissue structures.

Clearly, accurate patient-specific computer modeling of hyperthermia treatments to predict SAR distributions would be very useful for pretreatment evaluation of EM applicator setups. For example, Sathiaseelan *et al.* [8] used a 2-D numerical EM model to investigate the effect of phase steering with an annular phased array applicator system. The results of this numerical study were then used in the clinic to devise phase steering techniques to change the SAR patterns to improve the quality of treatments and reduce toxicity [9]. Also, patient-specific numerical simulation would enable parametric treatment studies to be performed quickly and inexpensively so that sensitive and insensitive parameters could be identified. These studies would also help to evaluate applicator-array systems now being developed.

Manuscript received July 20, 1990; revised August 1, 1991. This work was supported in part by American Cancer Society (Illinois Division) Grant 90-52, National Science Foundation Grant ASC-8811273, Office of Naval Research Contract N00014-88-K-0475, and Cray Research, Inc.

M. J. Piket-May, A. Taflove, W.-C. Lin, and D. S. Katz are with the Department of Electrical Engineering and Computer Science, McCormick School of Engineering, Northwestern University, Evanston, IL 60208.

V. Sathiaseelan and B. B. Mittal are with the Radiation Oncology Center, Northwestern Memorial Hospital, 250 East Superior, Room 44, Chicago, IL 60611.

IEEE Log Number 9105589.

A key step in realizing a computerized, patient-specific hyperthermia treatment planning involves the development of an accurate, efficient means for acquiring detailed 3-D anatomical tissue data for each patient. Regardless of the power of the EM analysis method, the modeling results can be no better than the tissue geometry data input. In principle, the advent of computed tomography (CT) has made the acquisition of accurate, patient-specific tissue geometry data feasible. However, processing the information from the CT data base to generate the corresponding 3-D dielectric medium data for the EM model can be difficult, especially if automation is desired to achieve speed. Problems include: 1) interpretation of the individual CT images to determine tissue and organ types and locations in each cross-section cut; and 2) interpolation or connection between adjacent CT images to reconstruct the original 3-D tissue geometry. The first issue is very complex, currently requiring the intervention of a human expert.

This paper describes progress made by our interdisciplinary group in both the EM modeling and CT-image interpretation problems. Section II reports the first analytical validations for 3-D computational EM models based on the finite-difference time-domain (FD-TD) method [10] for aperture-type hyperthermia applicators. These validations involve radiated fields from open-ended waveguides and horns, with benchmark data provided by the frequency-domain method of moments (MM). The validated FD-TD models of aperture sources are used later in Section IV for the patient-specific hyperthermia studies.

Section III describes the first automated CT image processing system to reconstruct patient-specific, 3-D tissue geometries for EM hyperthermia from serial CT image data. This novel system is based on sophisticated tools from the artificial intelligence, computer vision, and computer graphics disciplines [11]–[14]. It permits CT-based patient-specific hyperthermia models to be constructed without tedious manual contouring on digitizing pads or CRT screens. The system permits in principle near real-time assistance in hyperthermia treatment planning.

Section IV illustrates the entire process by describing automated 2-D and 3-D patient-specific models of EM hyperthermia of a human thigh due to a waveguide applicator. Here, the thigh tissue geometry data base is derived by combining 29 serial CT images of the patient. The FD-TD modeling results are shown as contour plots of the penetrating electric field and SAR. We find that different results are obtained from the 2-D and 3-D FD-TD models, and conclude that full 3-D tissue models are required for future clinical usage.

For completeness, we note that *two* distinct physical modeling problems are involved in the patient-specific computer simulation of hyperthermia treatments: 1) computation of the absorbed EM power distribution in tissue; and 2) the prediction of resulting temperature distributions using a suitable thermal model. These are two complex problems requiring different theoretical bases and different tissue property and physiological data. In this paper, only the patient-specific EM modeling problem is considered.

II. FD-TD Modeling Validations for Aperture Hyperthermia Sources

The important EM issues addressed in this paper are: 1) FD-TD modeling validations for aperture hyperthermia sources; and 2) 2-D versus 3-D modeling quantification. This section will focus on the first issue, while Section IV will consider the second. These are key areas to be investigated to ensure that EM modeling provides clinically meaningful answers, and to advance modeling progress in hyperthermia.

A. Background of EM Modeling

In the 1970's and early 1980's, 3-D predictive models of EM wave absorption by biological tissue structures were based largely on the frequency-domain method of moments (MM) using space-filling cubic [15] and tetrahedral [16] elements. Yet, because MM leads to systems of linear equations having dense, full, complex-valued coefficient matrices, the required computer resources prevented modeling of arbitrary 3-D structures spanning more than a few wavelengths. In fact, the literature indicates that the basic MM treatment of whole-body human tissue structures culminated in models having in the order of several hundred space cells, each of multicentimeter scale [17]. This resolution is inadequate to provide the details of internal tissue structure needed for patient-specific hyperthermia treatment planning.

Theoretical efforts therefore shifted to alternative formulations of MM which promise a dimensional reduction of computer resources. One such formulation [18] exploits the convolutional nature of the volume integral equation based on polarization currents to permit use of the fast Fourier transform (FFT). Although this extends MM modeling to structures having thousands of space cells, it may provide errors in SAR calculations for EM excitations having transverse electric field components [19]. This would greatly impede the application of FFT/MM approaches to the important 3-D tissue case.

An alternative to frequency-domain MM formulations was the FD-TD method introduced by Taflove in 1975 [20], [21], based in part on an algorithm published by Yee [22] in 1966. FD-TD is a direct finite-difference solution of Maxwell's time-dependent curl equations implementing a marching-in-time procedure which simulates the actual propagating EM waves by sampled-data numerical analogs. There is no need to set up or solve a system of linear equations. Thus, FD-TD computational resources are dimensionally low compared to MM. Furthermore, unlike the FFT/MM approaches, which also have dimen-

sionally low computer burdens, FD-TD has been shown to be robust, providing accurate modeling predictions for a wide variety of EM wave interaction problems in 2-D and 3-D [10]. A subset of these includes biological tissue interactions [19], [21], [23], including detailed (order 1-cm resolution) whole-human-body dosimetry under plane-wave illumination [24], and detailed partial- or whole-body hyperthermia modeling [25]–[27].

The increasing availability of Crays to the engineering EM community has permitted application of FD-TD to model EM wave interactions with arbitrary 3-D structures approximately ten times larger in electrical size than MM (1000 times larger in volume). At present, the largest and fastest reported 3-D FD-TD model is the jet engine inlet modeled by Katz and Taflove [28] for radar cross section. This model, implemented on the Cray Y-MP/8, spans 30 λ_o in 3-D, has a uniform $0.1 - \lambda_o$ resolution, and solves for *23-million* unknown vector field components. The Cray Y-MP/8 running time is only 3 min, *40 s* per illumination angle (1800 time steps—100 cycles of the incident wave—to the sinusoidal steady state).

In the area of EM wave interactions with biological tissue structures, the literature also indicates work in finite-element modeling [29], [30]. The goals of this work involve nearly conformal modeling of tissue structures using well-characterized finite-element geometry generation software. (FD-TD theory is also progressing in this area with the advent of accurate, fully conformal surface models based upon local Faraday's Law and Ampere's Law contour paths [31].) However, detailed studies [19], [23] have shown that simple FD-TD surface staircasing of cylindrical and spherical tissue structures is sufficient to permit calculation of the penetrating internal fields with a high degree of accuracy compared to the exact solutions. It is observed that FD-TD calculated fields penetrating a lossy dielectric structure show little sensitivity to the nature of the surface approximation of the structure. This observation permits effective use of simple staircasing FD-TD models for computing penetrating fields in tissue structures. These sacrifice little accuracy and have small computer burdens compared to the finite-element approaches.

B. FD-TD Validation Studies

At present, there exists only a limited set of validations of FD-TD models for clinically used hyperthermia applicators [25]–[27]. In this section, this paper provides the first analytical validations of FD-TD for generic aperture sources: open-ended waveguides and horns, including details of the waveguide probe excitation. Benchmark data are obtained from detailed frequency-domain integral equation and MM numerical results. These validation studies are relevant in that the patient-specific, FD-TD hyperthermia models to be discussed in Section IV employ similar 2-D and 3-D aperture sources; and it is clearly desirable to have confidence in the numerical EM model before drawing conclusions based upon the model (as we will).

Consider first the validation studies for the generic microwave aperture sources. Validation here consists of comparing the magnitude and phase of radiated near fields predicted by FD-TD and MM, and determining the level of disagreement. For example, Fig. 1a depicts the geometry of a 2-D waveguide-fed horn antenna, excited by a monopole probe, used for comparison of FD-TD and MM computed aperture electric field distributions. As seen in Fig. 1(b) and (c), the FD-TD and MM computations of radiated near fields agree within about 1% in magnitude and about 2° in phase. (This level of agreement has been found consistently for a variety of 2-D aperture sources.) This implies that the FD-TD predictions are, for engineering purposes, just as useful as those of MM.

Two analytical validation studies are considered for the 3-D FD-TD aperture source model. The first validation involves a simple rectangular waveguide radiating in free space. The waveguide is assumed to have a $2\lambda_o/3 \times \lambda_o/3$ cross section, and a $2\lambda_o$ length. A sinusoidally excited line source is assumed to be located $\lambda_o/3$ from the closed end, centered in the waveguide, and extending from the top to the bottom of the guide. The FD-TD computations for radiated far-fields are compared to those obtained using a standard electric field integral equation, triangular surface patching MM code with three different meshings, with results shown in Fig. 2. It is seen that the FD-TD predicted far-fields are "bracketed" by the various MM results, indicating a substantial code-to-code validation.

The second 3-D validation study compares FD-TD results to a recently published integral equation solution [32] for an infinitely long rectangular waveguide heating a planar, layered tissue medium. The waveguide of [32] is water-loaded ($\epsilon_w = 81\epsilon_0$), has a 5.6 × 2.8 cm cross-section, and is excited at 432 MHz. The tissue medium is comprised of a 0.5-cm skin layer ($\epsilon_s = (42 - j25)\epsilon_0$), a 1.0-cm fat layer ($\epsilon_f = (5 - j10)\epsilon_0$), and a muscle half-space ($\epsilon_m = (42 - j25)\epsilon_0$). For the FD-TD model, the waveguide is assumed to have finite length, 19.3 cm ($2.5\lambda_w$), with a line source located 1.9 cm ($0.25\lambda_w$) from the closed end. To maintain a reasonable FD-TD grid size, the infinite extent of the tissue structure is approximated by extending it only one-half skin depth in all directions from the waveguide. Overall, using a uniform 1.0-mm space resolution, the FD-TD grid size is 280 × 134 × 106 cubic cells (23.9-million vector field components).

Fig. 3 compares the FD-TD and integral equation results for penetrating electric field contours at the skin–fat interface 0.5 cm into the layered tissue structure. Because of symmetry in the x and y direction, only a single quadrant of the electric field distribution is shown for each z = constant plane. The agreement is quite good considering the truncated (noninfinite) tissue layers used in the FD-TD modeling.

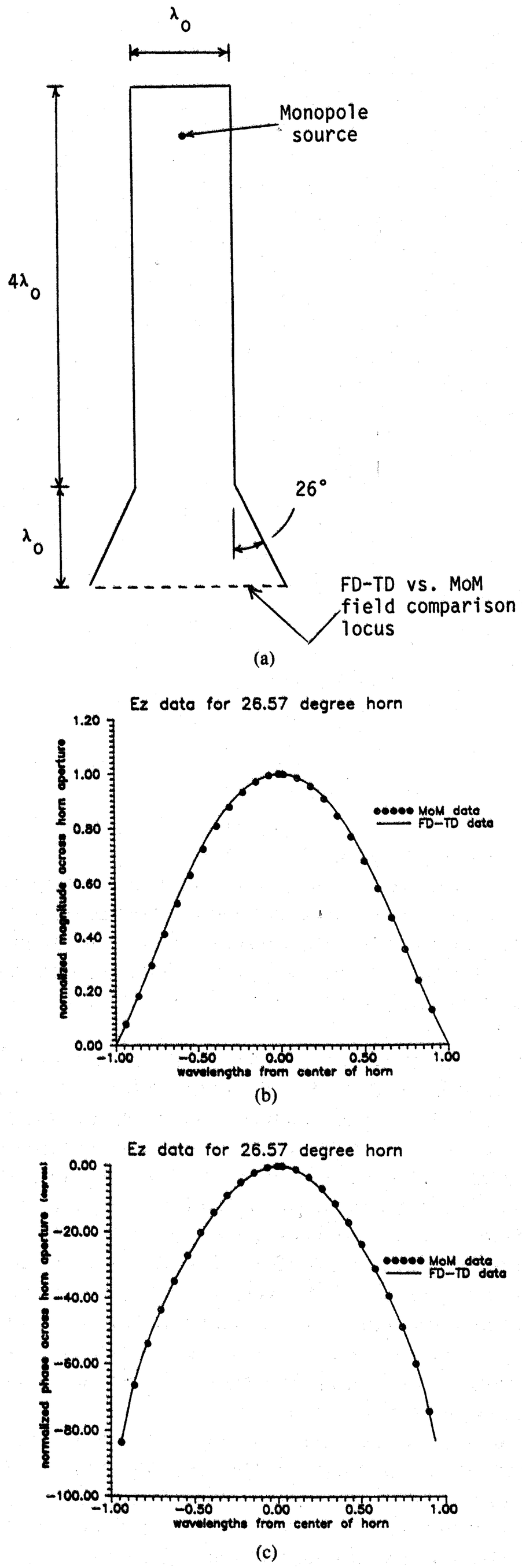

Fig. 1. 2-D waveguide-fed horn antenna: (a) Geometry, (b) electric field magnitude distribution at aperture, (c) electric field phase distribution at aperture.

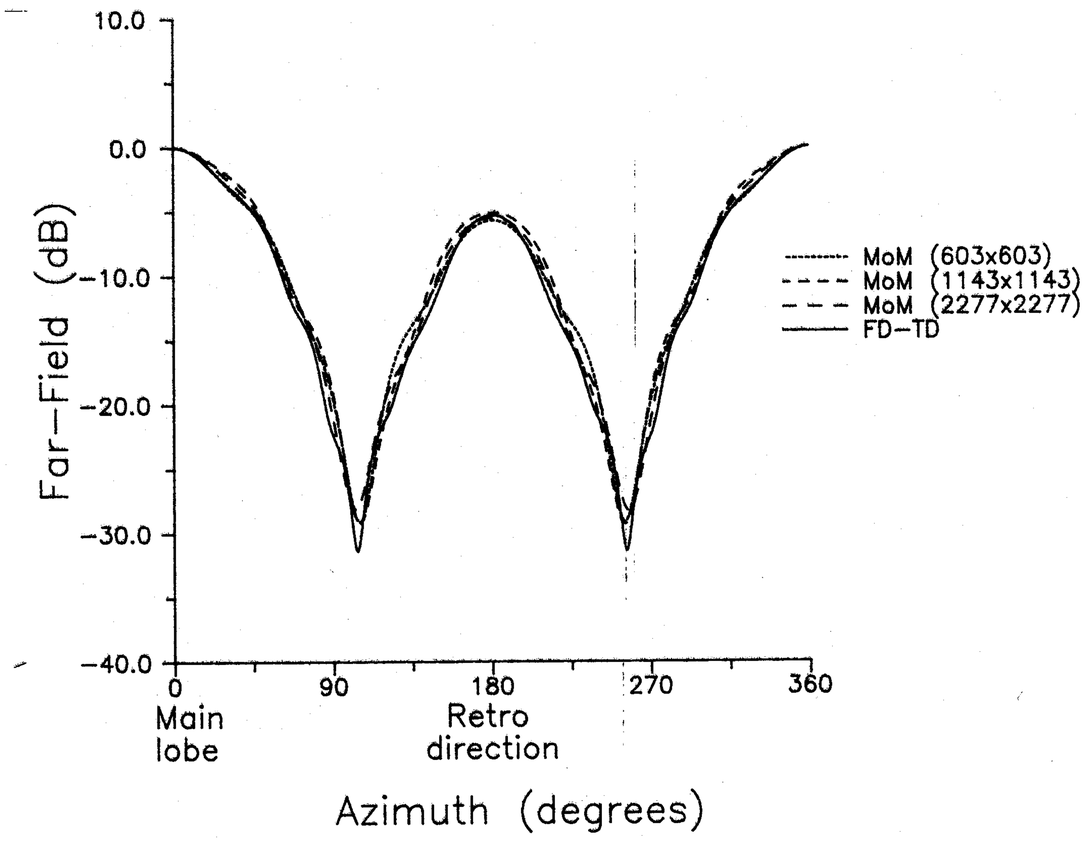

Fig. 2. Comparison of FD-TD and MM triangular surface patching results for the *H*-plane radiated far-field pattern of the short open-ended 3-D waveguide (various MM spatial resolutions).

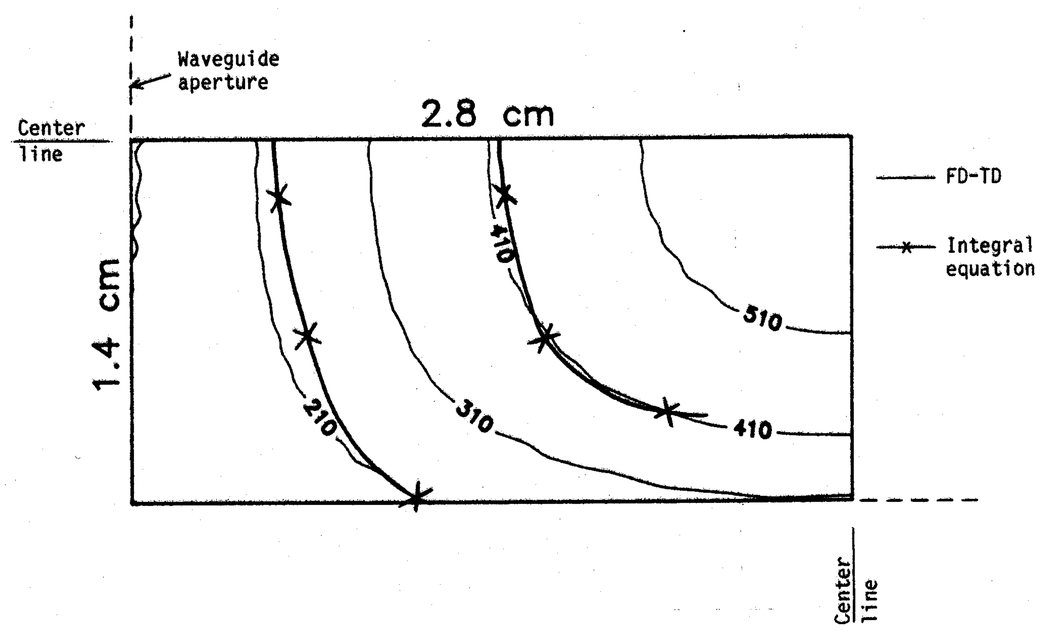

Fig. 3. Comparison of FD-TD and integral equation results [32] for penetrating electric field contours in a 3-layer tissue model due to a waveguide applicator. Location of map: 0.5 cm into the tissue (at the skin/fat interface); only one quadrant of the map is shown because of symmetry.

III. Automated CT Image Analysis and Reconstruction

A. Background

To reconstruct the 3-D tissue structure from serial CT cross-sectional image data, an image analysis system must perform two basic functions: 1) image segmentation/correspondence establishment; and 2) interpolation. *Image segmentation* is the process of dividing a CT image into regions that correspond to physical objects or parts [33]–[36]. After the meaningful entities in each slice have been identified (and their contours extracted), the next step is to establish the correspondence among them. By doing so, the information about the start contour in one slice and the corresponding goal contour(s) in adjacent slices can be obtained. There is no existing system that can perform fully automated medical image segmentation and correspondence establishment in a practical problem domain. *Interpolation* [11], [34], [37]–[39] ideally permits the re-

construction of the original tissue structure by filling the empty space between contours in adjacent CT slices derived by the segmentation process.

Much progress has been made during the past decade in addressing a similar problem in radiation treatment planning. Sophisticated computerized 3-D treatment planning systems based on CT and magnetic resonance imaging systems have been developed [40]–[44]. All of these systems use a combination of automatic and manual contouring methods to delineate tissue regions, i.e., segment images, in each CT slice. Edge-detection techniques have been used successfully to delineate structures that have significantly different Hounsfield numbers from those of adjacent tissues [44], [45]. A threshold CT value is selected and then the computer automatically traces a contour which separates points above and below the threshold.

However, for the spinal cord, brain stem, kidney, liver, stomach, heart, and other tissue structures embedded in fat or muscle tissue, the task is not straightforward. The Hounsfield CT numbers of these organs are sufficiently close to those of the surrounding tissue to make edge-detection algorithms useless, necessitating the use of a manual system. Here, the structures are outlined by skilled personnel having specific knowledge about the location of these organs, their shape, and their progression through the scanned volume as one moves from slice to slice through the CT data. Outlining is accomplished using a track-ball device or digitized pen system that controls the cursor on the computer screen.

Despite the development of graphical aids, manual generation of contours to delineate tissue structures can be tedious and labor-intensive, requiring many manhours to prepare the data for treatment planning. New approaches to define low-contrast tissues automatically or interactively have to be developed. This is an active area of research, and recently a technique for outlining regions where object CT values overlap has been reported [46]. However, to more fully automate this process, it will be necessary to use knowledge-based and other symbolic reasoning software tools.

Knowledge-based (expert) systems are an attempt to represent the knowledge, experience, and insight of the "expert" in a computer-based environment. These software tools have opened new paths for the use of computers in radiation oncology and diagnostic radiology [47]. For example, Pizer *et al.* [48] have recently developed a hierarchical figure-based shape description system with promising applications in defining low-contrast objects. Extension of these techniques to the needs of hyperthermia treatment planning offers the potential for new tools for tumor localization and extraction of anatomical features.

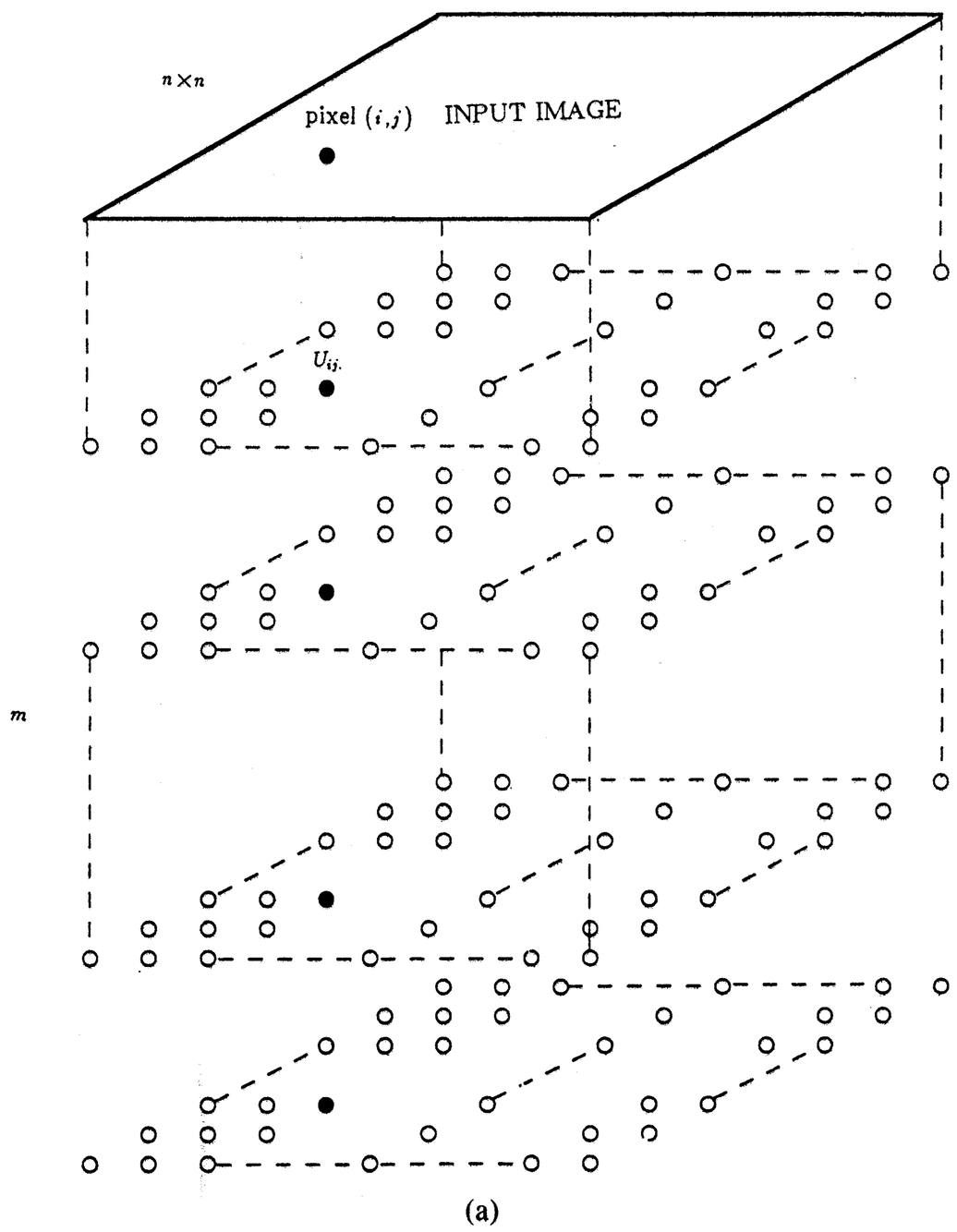

(a)

(b)

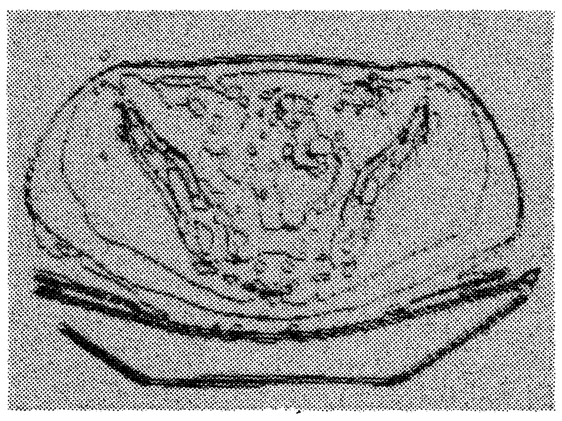

(c)

Fig. 4. Example of usage of constraint satisfaction neural network technique for automated segmentation of CT images: (a) Topology of the neural network, (b) CT image of pelvic cross section, (c) segmented image [14].

B. Our Approach

In this paper, we report the first highly automated CT image segmentation and interpolation scheme applied to model patient-specific EM hyperthermia. The method is based on the following:

1) Image Segmentation Using a Neural Network Approach: We report a constraint satisfaction neural

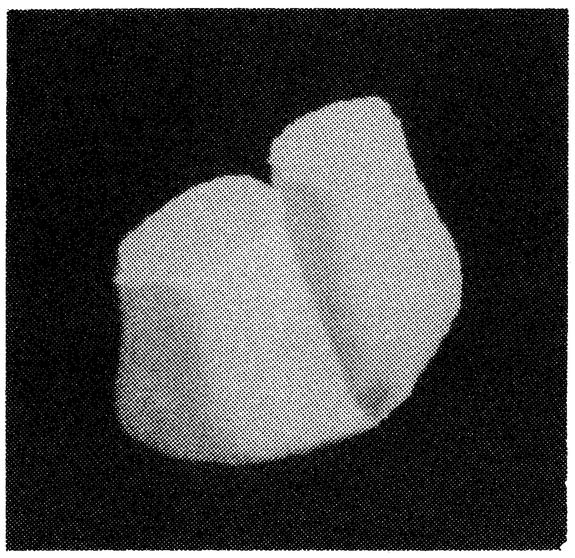

(a)

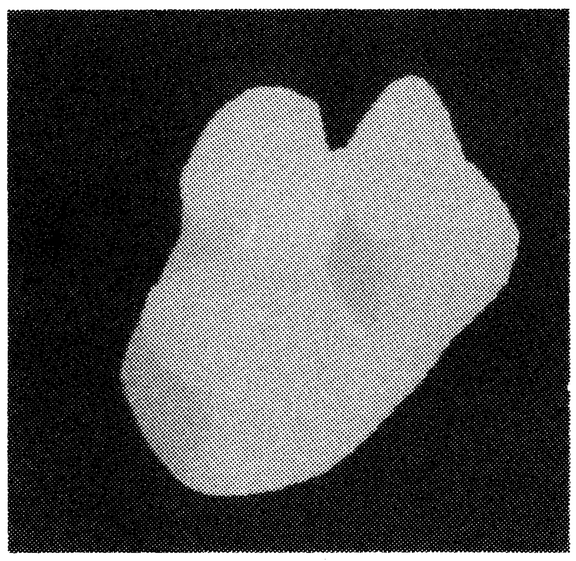

(b)

Fig. 5. Examples of usage of dynamic elastic surface interpolation technique for automated reconstruction of canonical 3-D branched objects from serial cross-sectional contours: (a) two branches, (b) three branches [11].

network[1] (CSNN) technique which enables, in principle, automatic segmentation of complex images [14]. In CSNN, each neuron corresponds to a pixel in an $n \times n$ image. Suppose that each pixel is to be assigned one of m labels. Then, the CSNN consists of $n \times n \times m$ neurons, and can be conceived as a 3-D array. The topology of the CSNN is shown in Fig. 4(a). The CSNN has been developed for image segmentation as the first step toward automated object reconstruction. Fig. 4(b) and (c) show an example of the use of the CSNN technique to automatically segment a CT image of a pelvic cross section [14] with results comparable to conventional techniques.

2) Interpolation: We also report the development of a dynamic elastic surface interpolation (DESI) scheme [11]–[13]. The central idea of DESI is to identify the geometric difference between the start and the goal contours, and derive force vectors that can be applied to the start contour to distort it to match the goal contour. The algorithm provides a mechanism to generate iteratively a series of intermediate contours for filling the gaps between the start and goal contours. A 3-D object is reconstructed by stacking up the start, intermediate, and goal contours. The major advantage of this method is its superior capability in handling the branching situation where a contour in one 2-D cut splits into several contours in adjacent cuts, or where several contours merge into one contour. DESI is simple and has the advantage that pairwise interpolation can be performed simultaneously with a parallel architecture. Fig. 5(a) and (b) show examples of the use of DESI to reconstruct canonical branched 3-D objects from serial cross-sectional contours [11].

[1]A neural network is composed of many interconnected processing elements that operate in parallel, and a weighted matrix of interconnections that allows the network to "learn" and "remember" [49]. Artificial neural networks are being used for a variety of applications including image and signal processing and pattern recognition. The parallel nature of a neural network permits, in principle, rapid concurrent processing of complex image data.

IV. Application to Patient-Specific EM Hyperthermia

We have applied the above techniques for the first time to interpret actual patient CT data for modeling EM hyperthermia. Specifically, we reconstructed a 3-D model of the human thigh from a collection of 29 serial CT images at 10 mm intervals. Two typical slices are shown in Fig. 6. Each slice consists of four different tissue structures: fat, muscle, bone, and bone marrow. In the reconstruction process, we assumed that we had the following prior knowledge:

1) Image content—each image contains a left and a right thigh.
2) Tissues types and spatial relationships—there are four types of tissues in each image, and if we draw a line from outside the whole region to its centroid, the order of regions encountered is always fat, muscle, bone, and then bone marrow.
3) Average intensity levels of the regions of different tissue types—used in thresholding operation.
4) Expected boundary between fat and muscle—should be smooth and closed, even though the muscle region may actually consist of many disconnected regions or may have bay-like (or crack-like) areas.

The four regions of interest corresponding to the four tissue types of the left thigh were obtained by the following semiautomatic procedure. First, the touching points of the two thighs were detected by locating the points with the maximum curvatures. Then, a line was drawn between the two points to separate the left thigh from the right thigh. The right thigh was blackened out and a 128 $\times$ 128 image [shown in Fig. 7(a)] containing only the left thigh was extracted. After manually analyzing this image to select three threshold values (see point 3), the pixels in the image were classified into groups by a thresholding operation. Fig. 7(b) shows the result of performing this operation on the image in Fig. 7(a). The boundaries between these regions were then obtained by automatic contour tracing methods [50]. Some heuristics were also applied[2] to obtain a closed and smooth boundary between fat and muscle (see point 4). After all the boundaries were detected, the four regions were labeled with distinct integers. Fig. 8 shows the results of Fig. 7 after boundary

[2]In our experiments, in an attempt to automate the boundary detection process, we also applied some well-recognized "signal-based" image segmentation algorithms such as split-and-merge [51] to this set of images. Although the algorithm had some success on some slices, it is not powerful enough to handle all the slices in our data set with a uniform set of parameters.

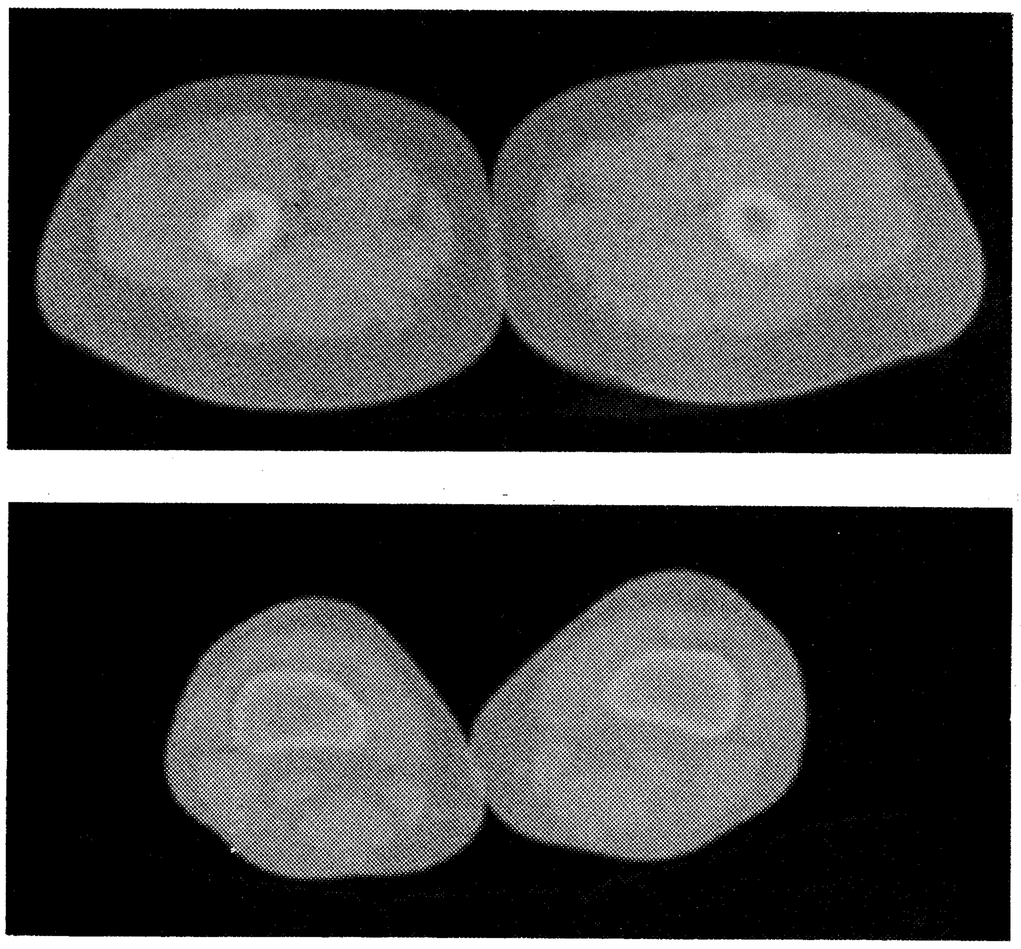

Fig. 6. Two typical CT images (slices) of the thighs of a patient.

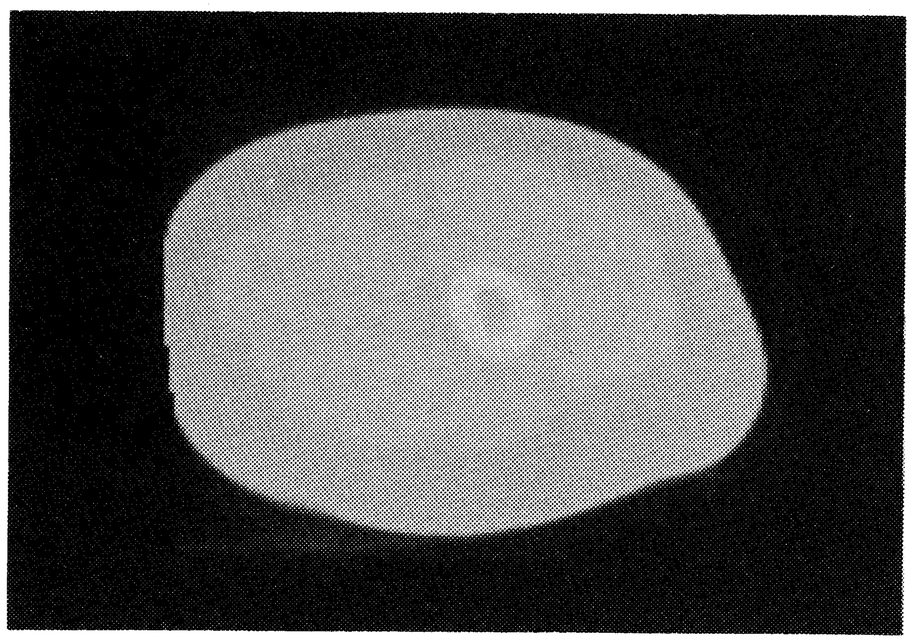

(a)

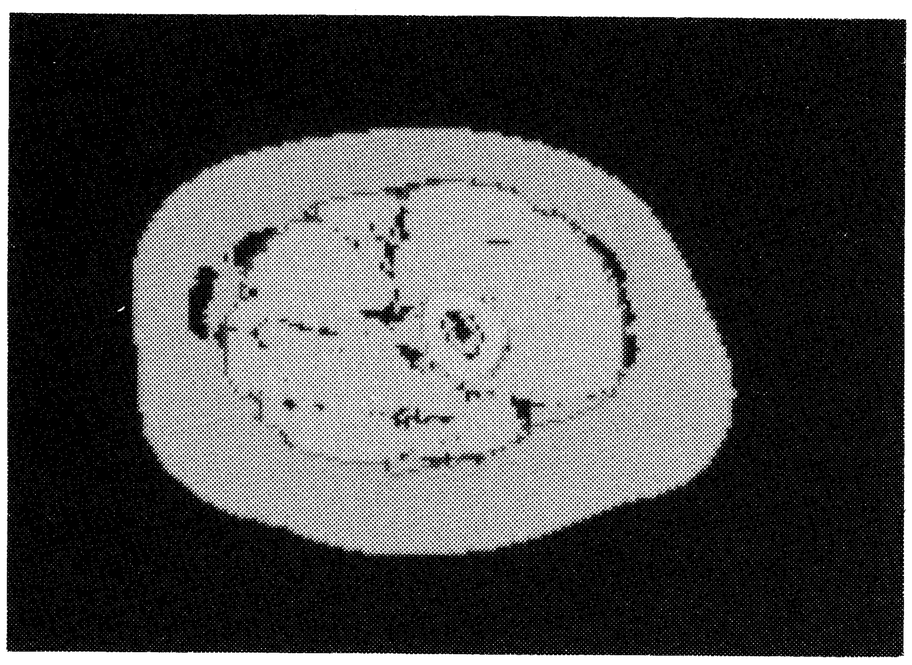

(b)

Fig. 7. Results of automated thresholding and pixel classification for the patient's left thigh of Fig. 6: (a) extraction of the left thigh, (b) results of processing.

detection and region labeling. The DESI method was then applied to each consecutive pair of slices for generating intermediate slices. After the pairwise interpolation, 28 intermediate slices were generated. Fig. 9 shows the result of stacking up the 57 slices.

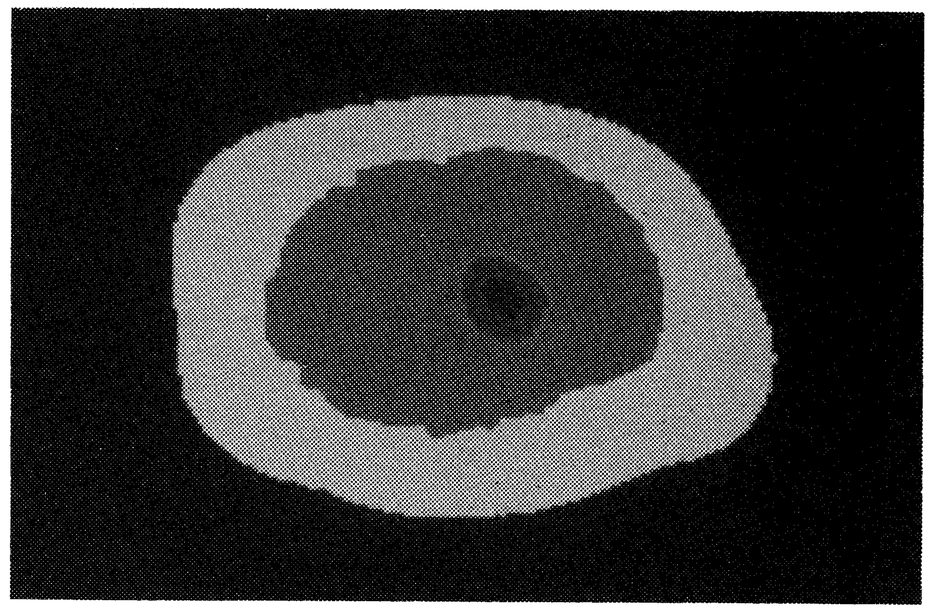

Fig. 8. Results of Fig. 7(b) after tissue boundary detection and region labeling.

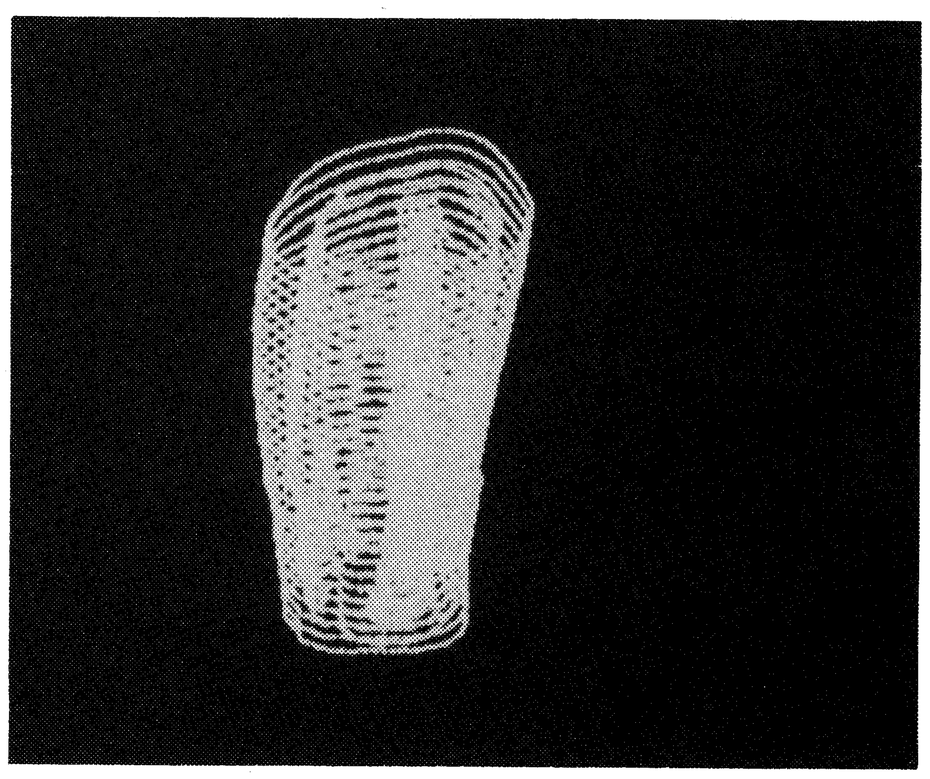

Fig. 9. Reconstructed 3-D thigh model (29 segmented CT images plus 28 intermediate slices generated using dynamic elastic surface interpolation).

A. 2-D Study

It was desired first to implement the prototype automated EM hyperthermia analysis system in 2-D. Using the CT-scan data of a human thigh, the tissue structure (fat, muscle, bone, and bone marrow) was automatically deduced as described above. A prototype automatic interface was constructed to take the data output of the CT analysis system and feed it into a Compaq 386/25/Weitek lab computer used for the 2-D FD-TD EM model. The model simulated a monopole-excited 2-D waveguide aperture source operating at 915 MHz as the hyperthermia applicator for the thigh, with and without a 1/4-wavelength slab used for impedance matching. (Previous studies discussed in Section II had validated the FD-TD model of the monopole-excited waveguide source.)

Fig. 10 depicts the 2-D geometry of the thigh and the 10×33.5 cm parallel-plate waveguide hyperthermia source operated at 915 MHz. A 150×300 cell FD-TD grid having a uniform resolution of 1.602 mm, the exact resolution of the CT data, was used for the model. The waveguide was assumed filled with a dielectric having $\epsilon_r = 6.0$ (except for a possible matching section having $\epsilon_r = 16.0$), and excited in the TE_1 mode by a line source centered within the guide 6.7 cm from the closed end. This provided an incident electric field parallel to the

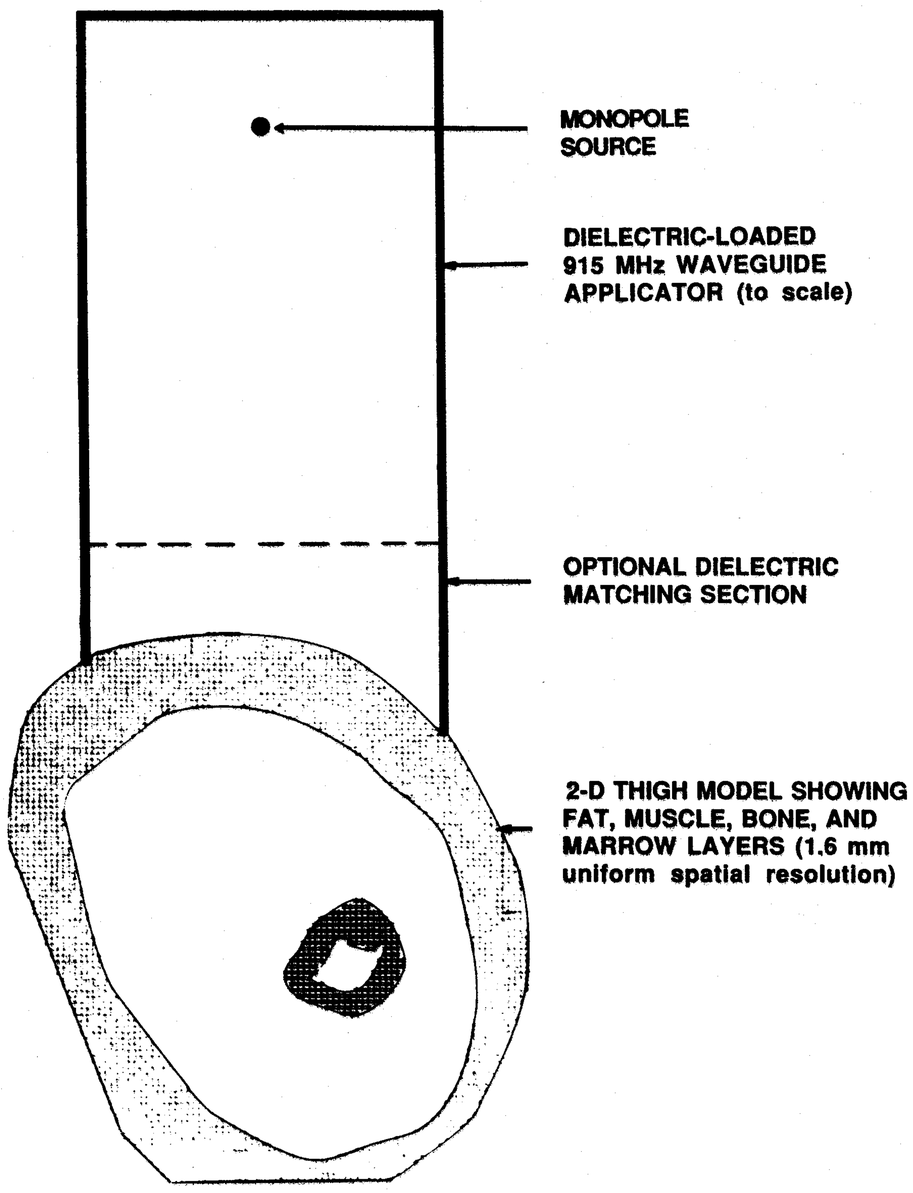

Fig. 10. Geometry of 2-D hyperthermia model, showing monopole-excited waveguide applicator and patient-specific thigh model, all contained within the FD-TD space grid.

thigh. Fig. 11(a) and (b) graph contour maps of the SAR distribution within the thigh for the unmatched and matched cases, respectively, normalized to 1000 W/m incident power. All data were obtained after time stepping eleven periods of the incident wave at 915 MHz (2 h run time on the Compaq). The figures clearly depict the matching action of the waveguide dielectric insert in enhancing EM heating within the thigh, and show an intense hot spot at the fat-muscle interface.

B. 3-D Study

Using the automated CT image analysis system to process 29 serial, patient-specific CT scans for the human thigh, we constructed a 3-D dielectric media data base which was automatically interfaced to a Cray-2 for the FD-TD model. (See Fig. 9 for the final 3-D thigh model.) The FD-TD grid resolution used here was 5 mm ($\lambda_d/27$). This resolution was chosen because it is the vertical distance between the interpolated CT layers. For the dielectric-loaded, TE_{10} mode waveguide hyperthermia applicator (dimensions 10 × 10 × 33.5 cm), the same metal and dielectric parameters as in the previous 2-D waveguide model were used, as well as the same excitation frequency. A line source, assumed to be centered in the guide 6.7 cm from the closed end, generated an incident electric field parallel to the thigh.

With the thigh in place, the FD-TD code solved for 2.4 million EM field components per time step. All data were obtained after time-stepping eleven periods of the incident wave at 915 MHz. (Eleven periods permits reasonable

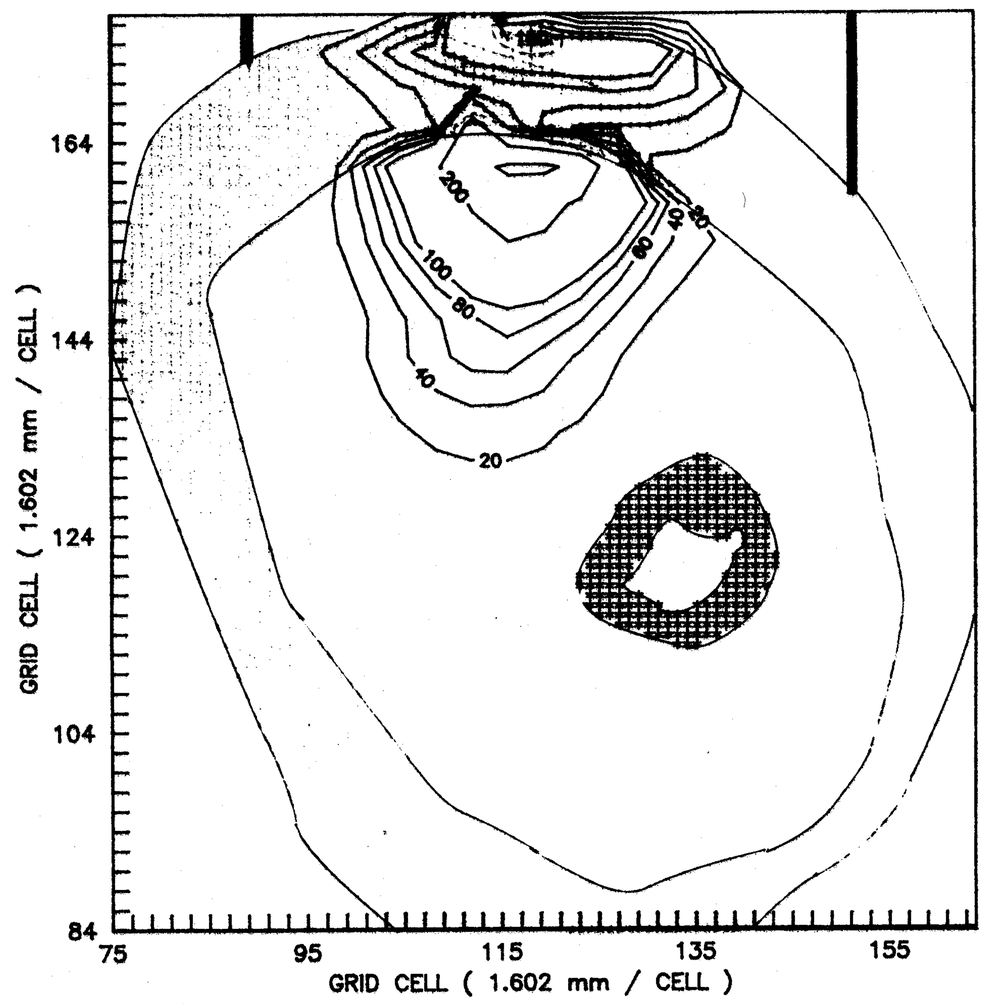

(a)

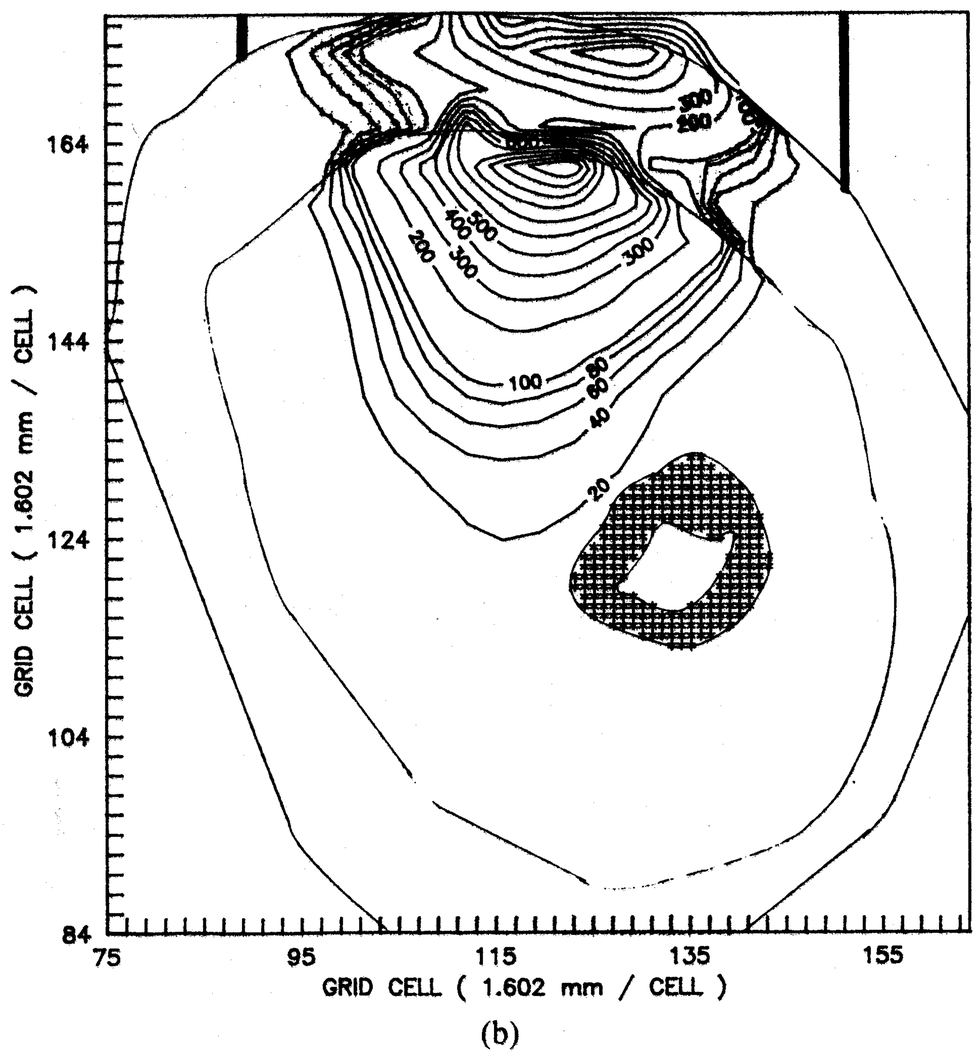

(b)

Fig. 11. FD-TD computed SAR distribution in the 2-D thigh model of Fig. 10, normalized to 1000 W/m incident power: (a) with no dielectric matching section, (b) with dielectric matching section.

convergence to the sinusoidal steady state for this case. During this time, a numerical wave can undergo one complete front-back-front traverse of the grid, taking into account the velocity-slowing effect of the high-permittivity tissue media.) This required 10 minutes of single-processor Cray-2 time per 3-D run. The previous 2-D model was also reworked in the same coarser resolution (5 mm) grid so that the 2-D and 3-D results could be directly compared. Fig. 12(a) shows the FD-TD computed SAR contour pattern penetrating into the 3-D model along a central horizontal cut, while Fig. 12(b) shows the corresponding FD-TD SAR contour pattern for the 2-D model.

We observe some interesting results which emphasize

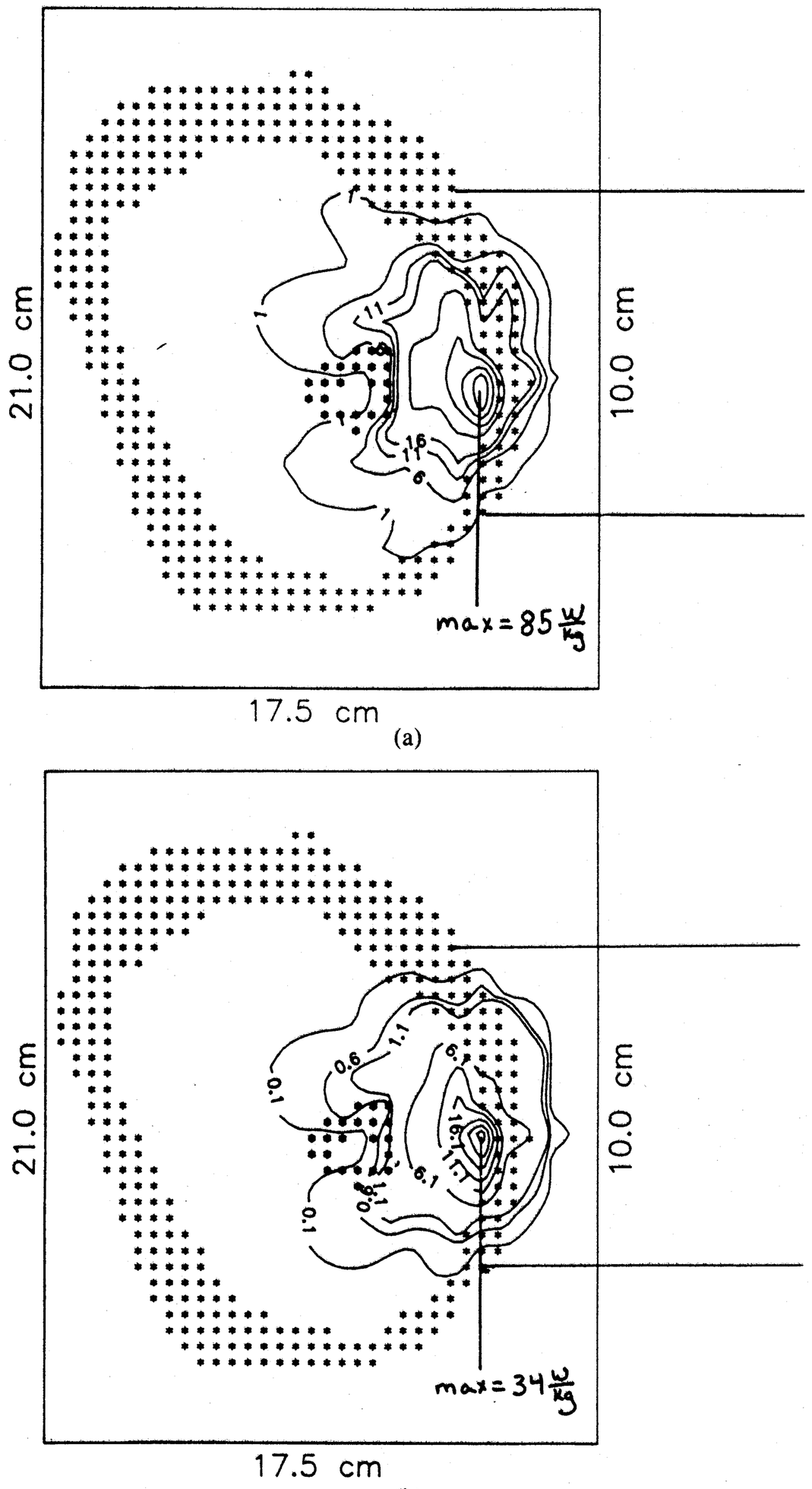

Fig. 12. FD-TD computed SAR distribution in the patient-specific thigh model, normalized to 1000 V/m incident waveguide field: (a) 3-D model, (b) 2-D model.

the need for 3-D EM modeling. With the same normalized incident electric field, deeper penetration is seen in the 3-D case. Note that the maximum SAR in the 3-D graph is 85 W/kg, whereas the maximum SAR in the 2-D graph is only 34 W/kg. If one compares the position of the 16 W/kg contour line in the 3-D and the 2-D graphs, the difference in penetration is clear. This contour almost penetrates the bone in the 3-D SAR graph, but is close to the fat–muscle interface in the 2-D SAR graph. This is perhaps one of the first comparisons of detailed computational modeling for EM absorption in 3-D versus 2-D.

To help explain the possibly counter-intuitive result that the 3-D model exhibits deeper penetration than the 2-D model, the electric field distribution through a vertical (z)

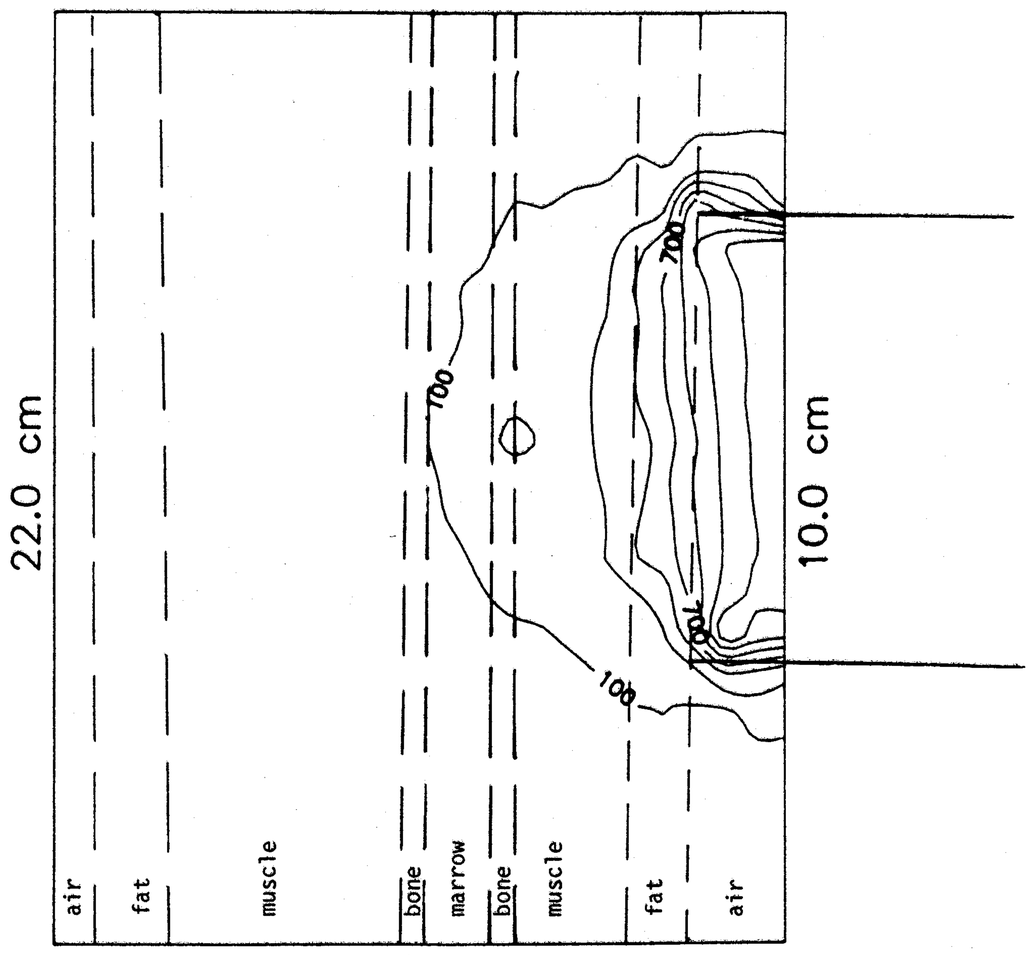

Fig. 13. FD-TD computed electric field map along a vertical slice of the 3-D patient-specific thigh model, at the waveguide center line (normalized to 1000 V/m incident waveguide field).

cut of the 3-D thigh geometry is shown in Fig. 13. Note the second curvature of the electric field contours in the third dimension, z. There is now a double curvature of the penetrating electric field, a sort of "bubble." This apparently bends the electric fields deeper into the thigh structure and sets up deeper heating.

V. Conclusion

This paper described progress by our group in automated computational modeling of patient-specific EM hyperthermia. We reported the first analytical validations of 3-D FD-TD models of aperture-type hyperthermia applicators. We also reported the first highly automated CT image segmentation and interpolation scheme applied to model patient-specific EM hyperthermia. We applied this technique to interpret actual patient CT data, reconstructing a 3-D model of the human thigh from a collection of 29 serial CT images at 10 mm intervals. Using FD-TD, we obtained 2-D and 3-D models of EM hyperthermia of this thigh due to a waveguide applicator. We found that different results are obtained from the 2-D and 3-D models, and concluded that full 3-D tissue models are required for future clinical usage.

References

[1] G. Arcangeli, J. Overgaard, D. G. Gonzalez, and P. N. Shrivastava, "Hyperthermia trials," *Int. J. Radiation Oncol. Biol. Physics*, vol. 14, suppl. 1, pp. S93–S109, 1988.

[2] R. Valdagni, F. Liu, and D. S. Kapp, "Important prognostic factors influencing outcome of combined radiation and hyperthermia," *Int. J. Radiation Oncol. Biol. Phys.*, vol. 15, pp. 959–972, 1988.

[3] J. L. Meyer, "The clinical efficacy of localized hyperthermia," *Cancer Res.*, vol. 44, pp. 4745S–4751S, 1984.

[4] J. Overgaard, "The current and potential role of hyperthermia in radiotherapy," *Int. J. Radiation Oncol. Biol. Phys.*, vol. 16, pp. 535–549, 1989.

[5] C. A. Perez and B. N. Emami, "Clinical trials with local (external and interstitial) irradiation and hyperthermia. Current and future perspectives," in *The Radiologic Clinics of North America*, R. A. Steeves, Ed. Philadelphia, PA: R. A. Saunders, vol. 27, 1989, pp. 525–542.

[6] C. A. Perez, B. Gillespie, T. Pajak, N. B. Hornback, B. N. Emami, and P. Rubin, "Quality assurance problems in clinical hyperthermia and their impact on therapeutic outcome: A report by the Radiation Therapy Oncology Group," *Int. J. Radiation Oncol. Biol. Phys.*, vol. 16, pp. 551–558, 1989.

[7] J. W. Hand and J. R. James, Eds., *Physical Techniques in Clinical Hyperthermia*. Research Studies Press, Letchworth, Herts., England, 1986.

[8] V. Sathiaseelan, M. F. Iskander, G. C. Howard, and N. M. Bleehen, "Theoretical analysis and clinical demonstration of the effect of power pattern control using the annular phased array hyperthermia system," *IEEE Trans. Microwave Theory Tech.*, vol. 34 (special issue on phased arrays), pp. 514–519, 1986.

[9] G. C. Howard, V. Sathiaseelan, G. A. King, A. K. Dixon, A. Anderson, and N. M. Bleehen, "Regional hyperthermia for extensive pelvic tumors using an annular phased array applicator: A feasibility study," *Brit. J. Radiol.*, vol. 59, pp. 1995–1201, 1986.

[10] A. Taflove, "Review of the formulation and applications of the finite-difference time-domain method for numerical modeling of electromagnetic wave interactions with arbitrary structures, (Invited Paper)," *Wave Motion*, vol. 10, pp. 547–582, 1988.

[11] W.-C. Lin, C.-C. Liang and C.-T. Chen, "Dynamic elastic interpolation for 3-D object reconstruction from serial cross-sectional images," *IEEE Trans. Med. Imag.*, vol. 7, pp. 225–232, 1988.

[12] W.-C. Lin, S.-Y. Chen, and C.-T. Chen, "A new surface interpolation technique for reconstructing 3-D objects from serial cross-sections," *Comp. Vis., Graph., Image Process.*, vol. 48, pp. 124–143, 1989.

[13] S.-Y. Chen, W.-C. Lin, C.-C. Chen, and C.-T. Chen, "Improvement on dynamic elastic interpolation for 3-D object reconstruction from serial cross-sectional images," *IEEE Trans. Med. Imag.*, vol. 9, pp. 71–83, 1990.

[14] W.-C. Lin, C.-K. Tsao, and C.-T. Chen, "Constraint satisfaction neural networks for image segmentation," *IEEE Trans. Neural Networks*, 1990.

[15] D. E. Livesay and K. M. Chen, "Electromagnetic fields induced inside arbitrarily shaped biological bodies," *IEEE Trans. Microwave Theory Tech.*, vol. 22, pp. 1273–1280, 1974.

[16] D. H. Schaubert, D. R. Wilton, and A. W. Glisson, "A tetrahedral modeling method for electromagnetic scattering by arbitrarily shaped inhomogeneous dielectric bodies," *IEEE Trans. Antennas Propagat.*, vol. 32, pp. 77–85, 1984.

[17] J. F. DeFord, O. P. Gandhi, and M. J. Hagmann, "Moment-method solutions and SAR calculations for inhomogeneous models of man with large number of cells," *IEEE Trans. Microwave. Theory. Tech.*, vol. 31, pp. 848–851, 1983.

[18] D. T. Borup and O. P. Gandhi, "Fast Fourier transform method for calculation of SAR distributions in finely discretized inhomogeneous models of biological bodies," *IEEE Trans. Microwave. Theory Tech.*, vol. 32, pp. 355–360, 1984.

[19] D. T. Borup, D. M. Sullivan, and O. P. Gandhi, "Comparison of the FFT conjugate gradient method and the finite-difference time-domain method for the 2-D absorption problem," *IEEE Trans. Microwave Theory Tech.*, vol. 35, pp. 383–395, 1987.

[20] A. Taflove and M. E. Brodwin, "Numerical solution of steady-state electromagnetic scattering problems using the time-dependent Maxwell's equations," *IEEE Trans. Microwave Theory Tech.*, vol. 23, pp. 623–630, 1975.

[21] ——, "Computation of the electromagnetic fields and induced temperatures within a model of the microwave-irradiated human eye," *IEEE Trans. Microwave Theory Tech.*, vol. 23, pp. 888–896, 1975.

[22] K. S. Yee, "Numerical solution of initial boundary value problems involving Maxwell's equations in isotropic media," *IEEE Trans. Antennas Propagat.*, vol. 14, pp. 302–307, 1966.

[23] D. M. Sullivan, D. T. Borup, and O. P. Gandhi, "Use of the finite-difference time-domain method in calculating EM absorption in human tissues," *IEEE Trans. Biomed, Eng.*, vol. 34, pp. 148–157, 1987.

[24] D. M. Sullivan, O. P. Gandhi, and A. Taflove, "Use of the finite-difference time-domain method in calculating EM absorption in man models," *IEEE Trans. Biomed. Eng.*, vol. 35, pp. 179–186, 1988.

[25] R. W. Lau, R. J. Sheppard, G. Howard, and N. M. Bleehen, "The modeling of biological systems in three dimensions using the time-domain finite-difference method: I. The implementation of the model; II. The application and experimental evaluation of the method in hyperthermia applicator design," *Phys. Med. Biol.*, vol. 31, pp. 1247–1266, 1986.

[26] C.-Q. Wang and O. P. Gandhi, "Numerical simulation of annular phased arrays for anatomically based models using the FD-TD method," *IEEE Trans. Microwave Theory Tech.*, vol. 37, pp. 118–126, 1989.

[27] D. Sullivan, "Three-dimensional computer simulation in deep regional hyperthermia using the finite-difference time-domain method," *IEEE Trans. Microwave Theory Tech.*, vol. 38, pp. 204–211, 1990.

[28] D. S. Katz and A. Taflove, "FD-TD visualization of electromagnetic wave interactions with three-dimensional objects," in *Proc. 1990 Int. Symposium, IEEE Antennas and Propagation Society/Int. Union of Radio Science*, Dallas, TX, May 1990.

[29] K. D. Paulsen, D. R. Lynch, and J. W. Strohbehn, "Three-dimensional finite, boundary, and hybrid element solutions of the Maxwell equations for lossy dielectric media," *IEEE Trans. Microwave Theory Tech.*, vol. 36, pp. 682–693, 1988.

[30] K. D. Paulsen and D. R. Lynch, "Time-domain solution of the Maxwell's equations by finite elements for electromagnetic hyperthermia," in *Abstracts of Papers for the Ninth Annu. Meet. North Amer. Hyperthermia Group*, Seattle, WA, Mar. 18–23, 1989, Abstract Ah-10.

[31] T. G. Jurgens, A. Taflove and K. R. Umashankar, "FD-TD conformal modeling of smoothly curved targets," *IEEE Trans. Antennas Propagat.*, to be published.

[32] K. S. Nikita and N. K. Uzunoglu, "Analysis of the power coupling from a waveguide applicator into a three-layered tissue model," *IEEE Trans. Microwave Theory Tech.*, vol. 37, pp. 1794–1801, 1989.

[33] R. M. Haralick and L. G. Shapiro, "Survey: Image segmentation techniques," *Computer Vis., Graph., Image Process.*, vol. 29, pp. 100–132, 1985.

[34] K. S. Fu and J. K. Mui, "A survey on image segmentation," *Pattern Recognit.*, vol. 13, pp. 3–16, 1981.

[35] E. M. Riseman and M. A. Arbib, "Survey: Computational techniques in the visual segmentation of static scenes," *Computer Graph. Image Process.*, vol. 67, pp. 253–261, May 1979.

[36] R. Nevaria, "Image segmentation," in *Handbook of Pattern Recognition and Image Processing*, vol. 29. T. Y. Young and K. S. Fu, Eds., 1985, pp. 100–132.

[37] H. Fuchs, Z. M. Kedem, and S. P. Uselton, "Optimal surface reconstrucion from planar surface contours," *Commun. ACM*, vol. 20, pp. 693–702, 1977.

[38] H. N. Christiansen and T. W. Sederberg, "Conversion of complex contour line definitions into polygonal element mosaics," *Computer Graphics*, vol. 12, pp. 187–192, 1978.

[39] J. D. Boissonnat, "Surface reconstruction from planar cross-sections," in *Proc. IEEE Conf. Computer Vision and Pattern Recognition*, San Francisco, CA, June 1985, pp. 393–397.

[40] P. Bloch and J. K. Udupa, "Application of computerized tomography to radiation therapy and surgical planning," *Proc. IEEE*, vol. 71, pp. 351–355, 1983.

[41] R. Mohan, G. Barest, L. J. Brewster, C. S. Chui, G. J. Kutcher, J. S. Laughlin, and Z. Fuks, "A comprehensive three-dimensional radiation treatment planning system," *Int. J. Radiation Oncol. Biol. Phys.*, vol. 15, pp. 481–495, 1988.

[42] B. A. Fraass and D. L. McShan, "3-D treatment planning: I. Overview of a clinical planning system," in *Proc. Ninth Conf. on the Use of Computers in Radiation Therapy*, Sceveningen, Netherlands. North Holland: Elsevier Science, 1987, pp. 273–276.

[43] J. A. Purdy, J. Wong, W. B. Harms *et al.*, "Three-dimensional radiation treatment planning," in *Proc. Ninth Conf. on the Use of Computers in Radiation Therapy*, Sceveningen, Netherlands. North Holland: Elsevier Science, 1987, pp. 277–279.

[44] M. Goitein and M. Abrams, "Multi-dimensional treatment planning: 1. Delineation of anatomy," *Int. J. Radiation Oncol. Biol. Phys.*, vol. 9, pp. 777–787, 1983.

[45] J. K. Udupa, "Interactive segmentation and boundary surface formation for 3-D digital images," *Computer Graphics and Image Processing*, vol. 18, 213–235, 1982.

[46] J. N. Roy, P. Steiger and C. C. Ling, "Overlap detection and contour-tracking algorithms for critical organs—application to kidney," *Computerized Med. Imag. Graph.*, vol. 13, pp. 153–161, 1990.

[47] S. Zink, "The promise of a new technology: Knowledge-based systems in radiation oncology and diagnostic radiology," *Computerized Med. Imag. Graph.*, vol. 13, pp. 282–293, 1990.
[48] S.M. Pizer, W. R. Oliver, J. M. Gauch, and S. H. Bloomberg, "Hierarchical figure-based shape description for medical imaging," in *Proc. NATO Advanced Science Institute on Mathematics and Computer Science in Medical Imaging.* New York: Springer-Verlag, 1988, pp. 365–387.
[49] J. L. McClelland and D. E. Rumelhart, *Explorations in Parallel Distributed Processing.* Cambridge, MA: MIT Press, 1987.
[50] T. Pavlidis, *Algorithms for Graphics and Image Processing.* Rockville, MD: Computer Science Press, 1982.
[51] S. L. Horowitz and T. Pavlidis, "Picture segmentation by a tree traversal algorithm," *J. Assoc. Comput. Mach.*, vol. 23, pp. 368–388, 1976.

Melinda J. Piket-May (S'89) was born in Kalamazoo, MI, on July 9, 1965. She received the B.S.E.E. degree from the University of Illinois, Urbana, in 1988, and the M.S. degree in electrical engineering from Northwestern University, Evanston, IL, in 1990.

She is currently pursuing the Ph.D. degree in the Department of Electrical Engineering at Northwestern University, where she works as Research Assistant. Her research interests include numerical modeling of electromagnetic phenomena with application to VLSI and biomedical problems.

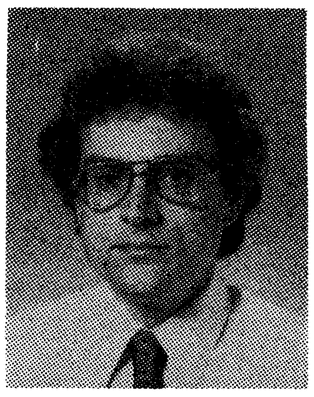

Allen Taflove (M'75–SM'84–F'90) was born in Chicago, IL, on June 14, 1949. He received the B.S. (with highest distinction), M.S., and Ph.D. degrees in electrical engineering from Northwestern University, Evanston, IL, in 1971, 1972, and 1975, respectively.

From 1975 to 1984, he was a staff member in the Electronics Division, IIT Research Institute, Chicago, IL, holding the positions of Associate Engineer, Research Engineer, and Senior Engineer. During this time, he was principal investigator on a number of externally funded programs, including five that contributed to the early development of the finite-difference time-domain method for computational modeling of electromagnetic wave interactions with complex structures. He was also a key contributor to large-scale programs involving the application of radio-frequency heating to produce oil in place (without mining) from deposits of oil shale, tar sands, and heavy oil; to accelerate oil production from slowly producing conventional wells; and to decontaminate large sections of the ground permeated with toxic chemical wastes. In this technical area, he has been awarded ten U.S. patents. He also authored a major EPRI report on electromagnetic field coupling effects of 60-Hz power transmission and distribution lines upon adjacent utilities. In 1984, he returned to Northwestern University where he is currently Professor of Electrical Engineering and Computer Science. He is actively pursuing supercomputing computational electromagnetics modeling of a broad variety of phenomena and technologies, including radiation and scattering, microwave/millimeter wave circuits, picosecond digital electronics, and femtosecond optical pulse propagation and switching. He also cooriginated and is active in Northwestern's innovative Honors Program in Undergraduate Research, wherein extremely bright high school graduates participate in an accelerated, research-enriched curriculum leading to the Ph.D. in as little as six years. In May 1991, he was honored as Adviser of the Year in the McCormick School of Engineering.

Dr. Taflove is a member of Tau Beta Pi, Eta Kappa Nu, Sigma Xi, Commission B of URSI, and the Electromagnetics Academy. During 1990–1991, he was a Distinguished National Lecturer for the IEEE Antennas and Propagation Society, and he is Chairman of the Technical Program of the 1992 IEEE Antennas and Propagation Society International Symposium to be held in Chicago. He is coauthor of the Best Paper at the 1983 IEEE International EMC Symposium, Washington, DC. He presented a one-hour invited talk at the AIAA 30th Aerospace Sciences Meeting, Reno, NV, Jan. 1992.

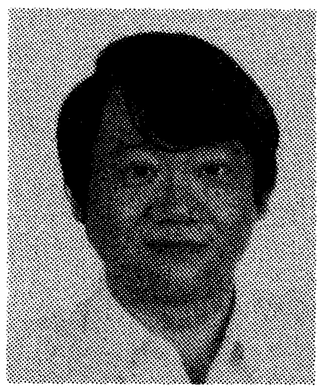

Wei-Chung Lin (S'80–S'84) received the B.S. degree in electrical engineering from the National Taiwan University, Taiwan, R.O.C., in 1975, the M.B.A. degree from the National Cheng-chi University in 1977, the M.S. degree in computer science from Michigan State University, East Lansing, in 1980, and the Ph.D. degree in electrical engineering from Purdue University, West Lafayette, IN, in 1984.

From 1984 to 1986, he was a Project Engineer in the R&D Center of the Standard Oil Company, Ohio. He is currently Assistant Professor of Electrical Engineering and Computer Science at Northwestern University and Faculty Member of the Center for Imaging Science at the University of Chicago. His current research activities include building computer vision systems for automated three-dimensional object recognition, expert vision systems for medical image understanding, and neural network systems for machine vision.

Dr. Lin is a member of AAAI, ACM, IEEE, INNS, SPIE, Classification Society of North America, and Pattern Recognition Society.

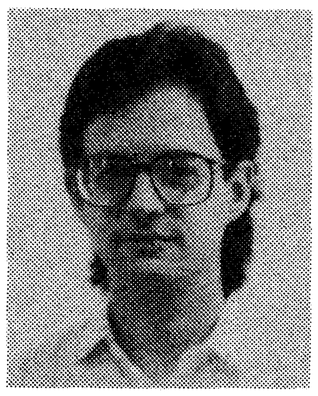

Daniel S. Katz (S'88) was born in Belleville, IL, on September 11, 1966. He received the B.S.E.E. and M.S. degrees in electrical engineering, both from Northwestern University, Evanston, IL, in 1988 and 1990, respectively.

Currently he is pursuing the Ph.D. degree in the Department of Electrical Engineering at Northwestern University, where he works as a Research Assistant. His research interests include computational modeling of electromagnetic wave propagation, radiation, and scattering.

Mr. Katz is a member of Tau Beta Pi and Eta Kappa Nu.

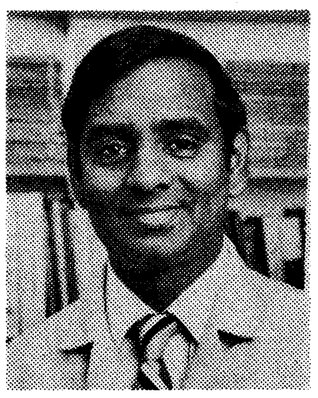

Vythialingam Sathiaseelan (M'86) was born in Sri Lanka in 1952. He received the B.Sc. degree in electronics engineering from the University of Sri Lanka, Katubadde Campus in 1976 with First Class honors and the Ph.D. degree in microwave engineering from the University of Bradford in 1982.

From 1982 to 1986, he was a Research Scientist with the Medical Research Council's Clinical Oncology and Radiotherapeutics Unit in Cambridge, England. He was an Assistant Professor in the Washington University School of Medicine, Mallinckrodt Institute of Radiology in St. Louis, USA from 1986 to 1988. He is currently employed by the Northwestern Memorial Hospital as Hyperthermia Engineer in the Radiation Oncology Center. He also holds an appointment as an Assistant Professor in Clinical Radiology in the Department of Radiology, Division of Radiation Oncology, Northwestern University Medical School. He is also a member of the Cancer Center, Northwestern University. His main research focuses on the development of improved electromagnetic techniques for heating deep-seated and superficial tumors and numerical modeling of electromagnetic interaction with biological objects.

Bharat B. Mittal was born in India in 1952. He received the B.S. degree in 1969 from Meerut University, India, and the M.B.B.S. degree from the Christian Medical College, Ludhiana, India in 1973.

He was a resident in Internal Medicine at the Christian Medical College, Ludhiana, India from 1975 to 1976 and in Radiation Oncology at the Northwestern University, Chicago, Illinois from 1977 to 1980. He had a Fellowship in Radiation Oncology from 1980 to 1981 at the Mallinckrodt

Institute of Radiology, Washington University School of Medicine, St. Louis, Missouri and was an Instructor of Radiation Oncology from 1981 to 1982 at the same institute. From 1982 to 1985 he was an Assistant Professor of Radiology, University of Pittsburgh, Pittsburgh, Pennsylvania. In 1985 he joined the Department of Radiology, Division of Radiation Oncology, Northwestern University Medical School, Chicago as a Clinical Assistant Professor of Radiology and became an Associate Professor in 1989. He is also a member of the Cancer Center, Northwestern University. He is a member of the attending medical staff of Northwestern Memorial Hospital, where he directs the hyperthermia program. His research involves management of head and neck cancers, lymphoid malignancies, and the use of hyperthermia with irradiation and/or chemotherapy in the treatment of a variety of malignant tumors.

Dr. Mittal is certified by the American Board of Radiology.